Geological Magazine

www.cambridge.org/geo

Early Jurassic (Toarcian) warming identified from lacustrine sediments of eastern Liaoning, China

Qian Zhang, Enpu Gong, Yongli Zhang and Changqing Guan

Resources and Civil Engineering College, Northeastern University, Shenyang 110819, Liaoning Province, China

Original Article

Cite this article: Zhang Q, Gong E, Zhang Y, and Guan C (2021) Early Jurassic (Toarcian) warming identified from lacustrine sediments of eastern Liaoning, China. *Geological Magazine* **158**: 1194–1208. https://doi.org/10.1017/S0016756820001235

Received: 26 September 2019
Revised: 16 August 2020
Accepted: 13 October 2020
First published online: 20 November 2020

Keywords:
Early Jurassic; Toarcian; climate warming; flora; organic carbon isotope; eastern Liaoning

Author for correspondence: Enpu Gong, Email: gongep@mail.neu.edu.cn

Abstract

This study focuses on the Tianshifu Basin, eastern Liaoning, China, which is filled with Lower–Middle Jurassic fluviolacustrine sediments rich in macroplants. Our aim is to explore the continental climate features of the late Early Jurassic period. The composition of the Early–Middle Jurassic flora and the carbon isotopic ratios of organic matter, total organic carbon, total organic nitrogen and sulphur of the rock samples from the Changliangzi section (the upper part of the Lower Jurassic deposits) have been investigated. Based on the flora, eastern Liaoning was generally characterized by temperate and humid conditions during the Early–Middle Jurassic period, but with rising temperatures during late Early Jurassic time. The sediments of the Changliangzi section show a transformation from shallow-lake facies to deep-lake facies. A positive organic carbon isotope excursion correlates with the deepening of this palaeolake, considered to be caused by climate warming. The late Early Jurassic climate warming indicated by floral and isotopic evidence corresponds to the climatic events recorded elsewhere in marine and continental sequences during the Toarcian Age, the so-called Toarcian Anoxic event, and may be associated with enhanced global greenhouse warming. This study provides new continental data supporting global warming during the late Early Jurassic period.

1. Introduction

The conditions of the Jurassic Period have been recognized as a typical example of a greenhouse climate (Berner & Kothavala, 2001; Jenkyns, 2003; Dera *et al.* 2011; Vajda *et al.* 2016). The abnormal environmental and climate conditions during late Early Jurassic time have long been a focus of geologists. In particular, this includes the Toarcian Oceanic Anoxic Event (T-OAE), first proposed in the 1980s (Jenkyns, 1985, 1988), which has been regarded as a significant global climatic and/or geological event with effects that have been observed worldwide (Al-Suwaidi *et al.* 2010; Han *et al.* 2018; Ruebsam *et al.* 2018). The responses of this global event primarily include the temporary and/or permanent disappearance of some marine biota (Palliani *et al.* 2002; Aberhan & Baumiller, 2003; Ruban, 2004; Erba *et al.* 2019; Ros-Franch *et al.* 2019), a rise in marine temperature (Jenkyns, 2003; Suan *et al.* 2008; Dera *et al.* 2009) and anomalies in geochemical indexes (McArthur *et al.* 2000; Kemp *et al.* 2005; Hesselbo & Pieńkowski, 2011).

The biotic, environmental and geochemical records of this global event are primarily based on marine sequences, while fewer studies have been conducted on continental sequences. Several phenomena of terrestrial ecosystems are believed to be responses to global warming during the late Early Jurassic period, such as alterations in the composition of the macroflora and palynoflora (Vakhrameyev, 1982, 1991; Wang *et al.* 2005), geochemical indexes that indicate an arid climate (Fu *et al.* 2017) and the enhancement of atmospheric partial pressure of CO_2 (pCO_2) (McElwain *et al.* 2005; Zhou *et al.* 2018). In fact, data from the terrestrial system not only supplement that of the marine system, but also provide more accurate climate fluctuation records and highlight differences between continental and oceanic responses to global warming. For example, the early stages of volcanogenic global warming were more severe for the terrestrial ecosystem than the marine ecosystem, and changes in the diversity and composition of plants were initially more rapid in the terrestrial ecosystem (Slater *et al.* 2019). Nevertheless, an understanding of the effect of global warming on the continents is currently insufficient and incomplete compared with that of the ocean.

The Chinese Jurassic strata are dominated by terrestrial sequences, providing favourable materials for the study of the Jurassic palaeoenvironment and palaeoclimate. This study focuses on the Tianshifu Basin, eastern Liaoning, China, which is filled with Lower–Middle Jurassic fluvial and lacustrine sediments and is rich in plant fossils (Liaoning Bureau of Geology and Mineral Resources, 1989; Xu *et al.* 2003). To explore the continental climate features of the late Early Jurassic period, the flora and geochemical features were studied by investigating the evolutionary trend of the flora (based on macro-plant fossils) as well as by analysing the isotopic ratios

CAMBRIDGE UNIVERSITY PRESS

of organic carbon ($\delta^{13}C_{org}$), total organic carbon (TOC), total nitrogen (TN) and total sulphur (TS) in the rock samples.

2. Geological setting

The Tianshifu Basin is a small-scale faulted basin that covers an area of *c.* 12.5 km^2 and is located on the NE edge of the North China Plate (Fig. 1a, b). The basin is filled with Lower–Middle Jurassic fluvial and lacustrine sediments that can be divided into the Beimiao and Changliangzi formations (Lower Jurassic) and the Zhuanshanzi, Dabu and Sangeling formations (Middle Jurassic) (LBGMR, 1989; Xu *et al.* 2003).

In complete contrast to the relatively stable tectonic background of the periods prior to the Mesozoic, a series of NE faults and folds began to form in the Mesozoic in eastern China, the formation of which was accompanied by intense volcanic activity and magmatic intrusion under the impact of the NW subduction of the Palaeo-Pacific Plate. In general, eastern Liaoning experienced a period of long-term uplift and suffered intense weathering and denudation during the Jurassic period. Several small-scale inland lake basins, including the Tianshifu Basin, were formed exclusively in faulted and lowland areas (LBGMR, 1989; Wu *et al.* 2007*b*).

The Changliangzi Formation, which is also known as Changliangzi Black Shale, is primarily exposed in the north and SW of the Tianshifu Basin (Fig. 1c). The age of the Changliangzi Formation is generally considered to be late Early Jurassic, based on faunal and floral characteristics (Zheng & Zhang, 1990*a*, *b*). In addition, the Lower–Middle Jurassic strata in eastern Liaoning can be compared with that in western Liaoning in terms of lithological character, fossils and unconformity formed in the regional tectonic movement (Fig. 2) (Xu *et al.* 2003). The Beipiao Formation in western Liaoning is considered to be contemporaneous with the Changliangzi Formation in eastern Liaoning (Xu *et al.* 2003). It is also thought that the underlying Xinglonggou Formation formed during the Early Jurassic period (Shao & Yang, 2008) and the overlying Haifanggou Formation, which is contemporaneous with the Zhuanshanzi and Dabu formations, formed during Middle Jurassic time (Chang *et al.* 2014). The age of the Beipiao Formation in western Liaoning, that is, the Changliangzi Formation in the Tianshifu Basin, is therefore considered to be late Early Jurassic (Toarcian).

The Changliangzi Formation consists of an association of fluvio-lacustrine clastic sediments that can be divided into two parts: the lower part is dominated by conglomerates, sandstone and siltstone and is intercalated with shale and coal intervals, and the upper part is composed of black shale and siltstone that contains several sandstone layers (LBGMR, 1989; Xu *et al.* 2003). The upper part of the Changliangzi Formation is well-preserved in the study region, but the lower part is absent as a result of tectonic movement and human activities. Nevertheless, the Changliangzi Formation in the study area can still provide useful material to research the continental palaeoclimate and palaeoenvironment of the late Early Jurassic period.

3. Materials and methods

Rock samples were collected throughout the Changliangzi section in the SW Tianshifu Basin (Fig. 1c), and a total of 76 samples, with approximate average weight 500 g each, were obtained from an outcrop using a geological hammer. From the 76 rock samples, including sandstone, siltstone, mudstone and shale, 36 fine-grained samples, which may contain more organic matter (OM), were selected and prepared for geochemical analyses (Fig. 3). The samples were washed with distilled water using a supersonic cleaner to remove superficial contaminants, dried, crushed into small fragments and then ground into a powder.

TOC and TS analyses of the 36 samples were conducted using a Leco-344 automatic carbon and sulphur analyser at the Lanzhou Center for Oil and Gas Resources, Institute of Geology and Geophysics, Chinese Academy of Sciences. Prior to testing, the powdered samples were treated with 5% HCl for 24 hours to remove inorganic carbon, rinsed repeatedly with deionized water until the pH of the liquid was neutral, and then dried. TN analyses were conducted using an EA 3000 elemental analyser at the Nanjing Institute of Geography and Limnology, Chinese Academy of Sciences.

In addition, $\delta^{13}C_{org}$ was analysed using a MAT 253 mass spectrometer at the Lanzhou Center for Oil and Gas Resources. Prior to these analyses, powdered samples weighing 0.1–1 g were dissolved in 50 mL of 5% HCl, heated until one-third of the volume remained, and subsequently rinsed repeatedly with deionized water until the pH of the liquid became neutral. Samples were then dried at 40–60°C for 12 hours prior to analyses, and results were determined in accordance with the PDB standard.

A total of 44 plant macrofossils were collected from three areas: those from the upper part of Changliangzi Formation (late Early Jurassic) come from a gully in the west of Yaobu village, and those from the Dabu Formation (Middle Jurassic) come from a road slope to the NE of the town of Tianshifu and from a coal gangue pile to the SE of Tianshifu town (Fig. 1c).

It must be stated that the isotopic record is only from the Changliangzi section (the upper part of the Changliangzi Formation, late Early Jurassic). Moreover, the plant macrofossils collected from the upper part of the Changliangzi and Dabu formations are from an unknown horizon and are not constrained by isotopic results.

4. Results

4.a. Petrography and sedimentary environment

The examined section of the Changliangzi Formation has a thickness of *c.* 230 m, containing a succession of shale, siltstone and sandstone. The middle to lower part of this section (*c.* 0–167 m) is primarily composed of grey-green siltstone and black shale interrupted by occasional intervals of grey-yellow fine and coarse sandstone (Fig. 4a). The siltstone and fine sandstone are generally thin-bedded (*c.* 5–20 mm) and contain sporadic stalk fragments and abundant well-preserved bivalves (Fig. 4b–d). Consecutive or non-consecutive bedding composed of grey-yellow fine sand and black clay is found in unfossiliferous fine sandstone, which sometimes has faulted lamina and a sand-ball structure (Fig. 4e, f). In contrast with the fine sandstone, the interval of the coarse sandstone is thicker (*c.* 10–20 cm), has a massive structure, and is marked by poorly sorted and angular grains of quartz, feldspar and rock debris with tiny mineral and clay filling interstices (Fig. 4g). The uppermost Changliangzi section (at a height of *c.* 167–230 m) is dominated by black shale with nearly no siltstone or sandstone intervals. There are a few phytoclasts but no benthic fossils; however, black OM with a residual plant structure was identified (Fig. 4h).

The sedimentological and petrographic characteristics of the strata of the Changliangzi section are indicative of lacustrine facies. The low-maturity sandstone and large numbers of benthic organisms in the middle to lower part of the section are interpreted as having formed in a shallow lake near an eroding upland. In contrast, the pure-black shale rich in OM in the uppermost part of the section suggests deeper lake conditions. This deepening lacustrine

https://doi.org/10.1017/S0016756820001235 Published online by Cambridge University Press

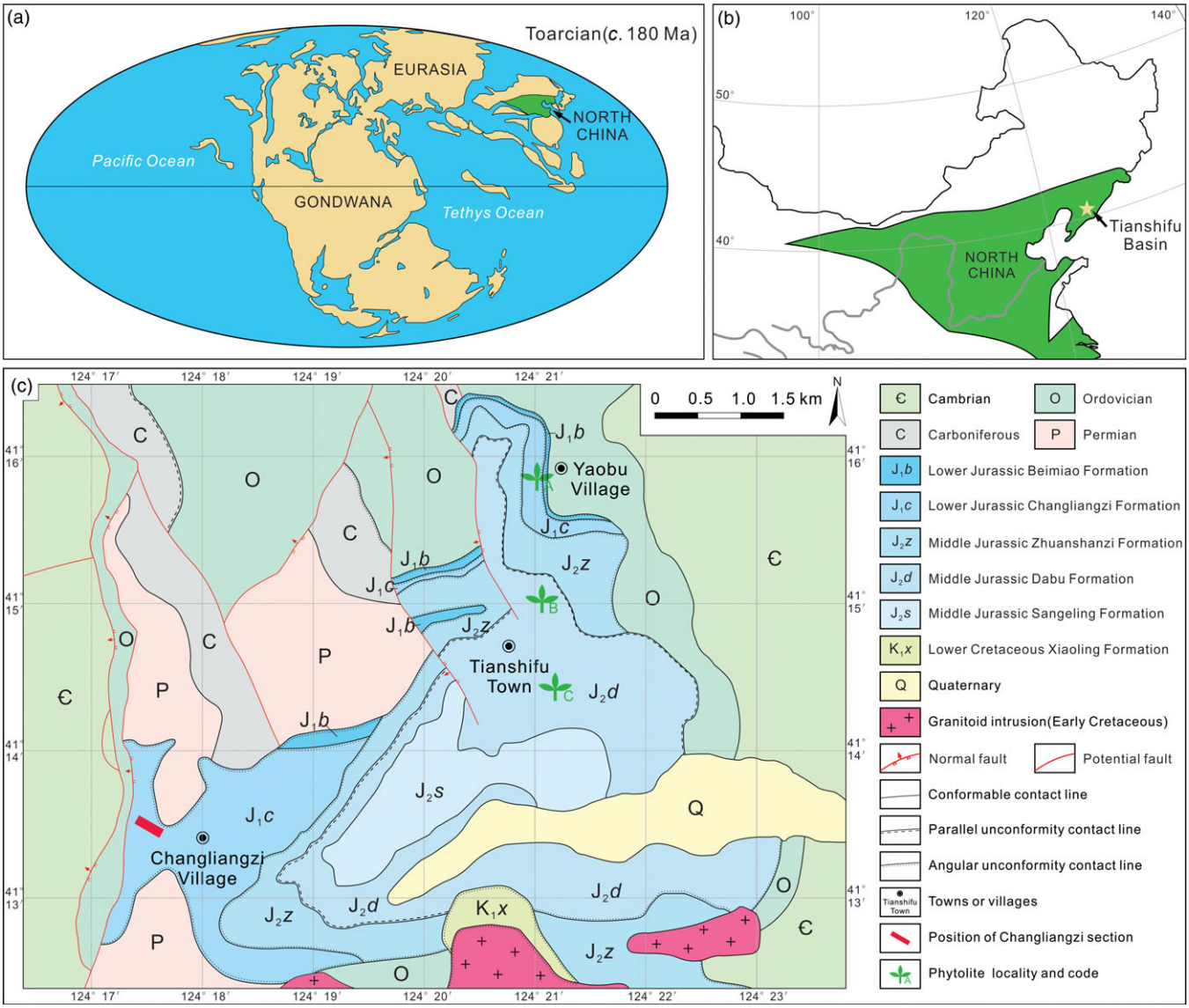

Fig. 1. (Colour online) (a) Palaeogeographic map of the late Early Jurassic period, redrawn after Scotese (2004); (b) location of the Tianshifu Basin (the yellow star indicates the study area); and (c) generalized geological map of the Tianshifu Basin. Location of the Changliangzi section and phytolite are presented.

sequence is consequently well-represented in the Changliangzi section within the Tianshifu Basin.

4.b. Flora

The Tianshifu Basin is rich in Early and Middle Jurassic plant fossils, and we identified a total of 17 genera and 37 species of plant macrofossils collected from the upper part of the Changliangzi Formation and the Dabu Formation (Table 1, Figs 5, 6).

The plants of the upper part of the Changliangzi Formation (late Early Jurassic) were collected in a gully to the west of the village of Yaobu (Fig. 1c, phytolite locality (PL-) A) and include 10 genera and 16 species. This flora is dominated by ferns, which make up half of the total number of plants, and contain Dicksoniaceae, Osmundaceae and Schizaeaceae. Dicksoniaceae (25%) dominates and mainly includes *Coniopteris*. Osmundaceae accounts for 19% and consists of *Cladophlebis* and *Todites*. Schizaeaceae (6%) is relatively rare and is composed of *Klukia*. The second-most abundant representatives of this flora are the sphenopsids (25%), including *Equisetites* (19%) and *Neocalamites* (6%). Cycadophytes occur and make up 13%, represented by *Pterophyllum* and *Nilssonia*. In addition, both ginkgophytes and conifers contribute only 6% and are represented by *Baiera* and *Podozamites*, respectively (Fig. 7a).

The plants of the Dabu Formation (Middle Jurassic) were collected from a road slope to the NE of the town of Tianshifu (Fig. 1c, PL-B) and from a coal gangue pile to the SE of the town of Tianshifu (Fig. 1c, PL-C), and include 16 genera and 28 species. This flora has a higher diversity but is still characterized by the predominance of ferns (36%), which include Osmundaceae, Dicksoniaceae and Marattiaceae. Osmundaceae accounts for 18% and still includes *Cladophlebis* and *Todites*. Dicksoniaceae decreases to 14% and is composed of *Coniopteris* and *Dicksonia*. Marattiaceae replaces Schizaeaceae with a lower content of 4%, and is represented by *Marattiopsis*. Ginkgophytes (25%) have a higher content and diversity than in the Changliangzi Formation, including *Baira* and *Sphenobaiera* together with *Sphenarion*, *Ginkgo* and *Czekanowskia*. Sphenopsids account for 18% and are represented by *Equisetites* (11%) and *Neocalamites* (7%). The number and species of cycadophytes

https://doi.org/10.1017/S0016756820001235 Published online by Cambridge University Press

SERIES	EASTERN LIAONING				WESTERN LIAONING			
	Lithostratigraphic units		Lithologic character	Fossil	Lithostratigraphic units		Lithologic character	Fossil
MIDDLE JURASSIC	Dabu formation	Upper part	Shale and siltstone, intercalated with sandstone and coal intervals	**PLANTS**: *Coniopteris simplex-Williamsoniella burecovae* assemblage **BIVALVES**: *Unio* cf. *balbinesis* **OSTRACODA**: *Darwinula magna*	Haifanggou formation	Upper part	Conglomerates, intercalated with tuff	**PLANTS**: *Coniopteris simplex-Eboracia lobifolia* assemblage **BIVALVES**: *Ferganoconcha haifanggouensis* **CONTROSTRACA**: *Euestheria haifanggouensis* **INSECTS**: *Samarura* ? sp.
		Lower part	Conglomerates and sandstone, intercalated with shale and siltstone			Middle part	Sandstone, siltstone, shale, intercalated with conglomerates	
	Zhuanshanzi formation	Upper part	Sandstone and shale, intercalated with coal intervals	**PLANTS**: *Coniopteris simplex-Eboracia lobifolia* assemblage		Lower part	Conglomerates, intercalated with sandstone, shale and tuff	
		Lower part	Conglomerates, intercalated with sandstone and shale					
LOWER JURASSIC	Changliangzi formation	Upper part	Black shale and siltstone, intercalated with sandstone	**PLANTS**: *Dictyophyllum nathorsti-Cladophlebis asiatica* assemblage **BIVALVES**: *Pseudocardinia curta-Tutuella chachlovi* assemblage **OSTRACODA**: *Darwinula longovata-D. taochunensis* assemblage	Beipiao formation	Upper part	Black shale and siltstone, intercalated with sandstone	**PLANTS**: *Thaumatopteris-Cladophlebis* assemblage **INSECTS**: *Rhipidoblattina longa-Euryblattula chaoyangensis* assemblage
		Lower part	Conglomerates, sandstone and siltstone, intercalated with shale and coal intervals			Lower part	Sandstone and siltstone, intercalated with conglomerates and mudstone	**PLANTS**: *Dictyophyllum nathorsti-Cycadocarpidium tricarpus* assemblage **INSECTS**: *Taublatta yangshugouensis-Rhipidoblattina lonqa* assemblage
	Beimiao formation		Tuff, andesite, and greywacke		Xinglonggou formation		Andesite and basalt, intercalated with sandstone, siltstone	**PLANTS:** *Neocalamites* sp., *Equisetum* sp., *Cladophlebis*

Fig. 2. Stratigraphic correlation of Lower–Middle Jurassic strata between eastern and western Liaoning, after Xu *et al*. (2003). The wavy lines and the dotted lines represent angular unconformity contacts and parallel unconformity contact, respectively.

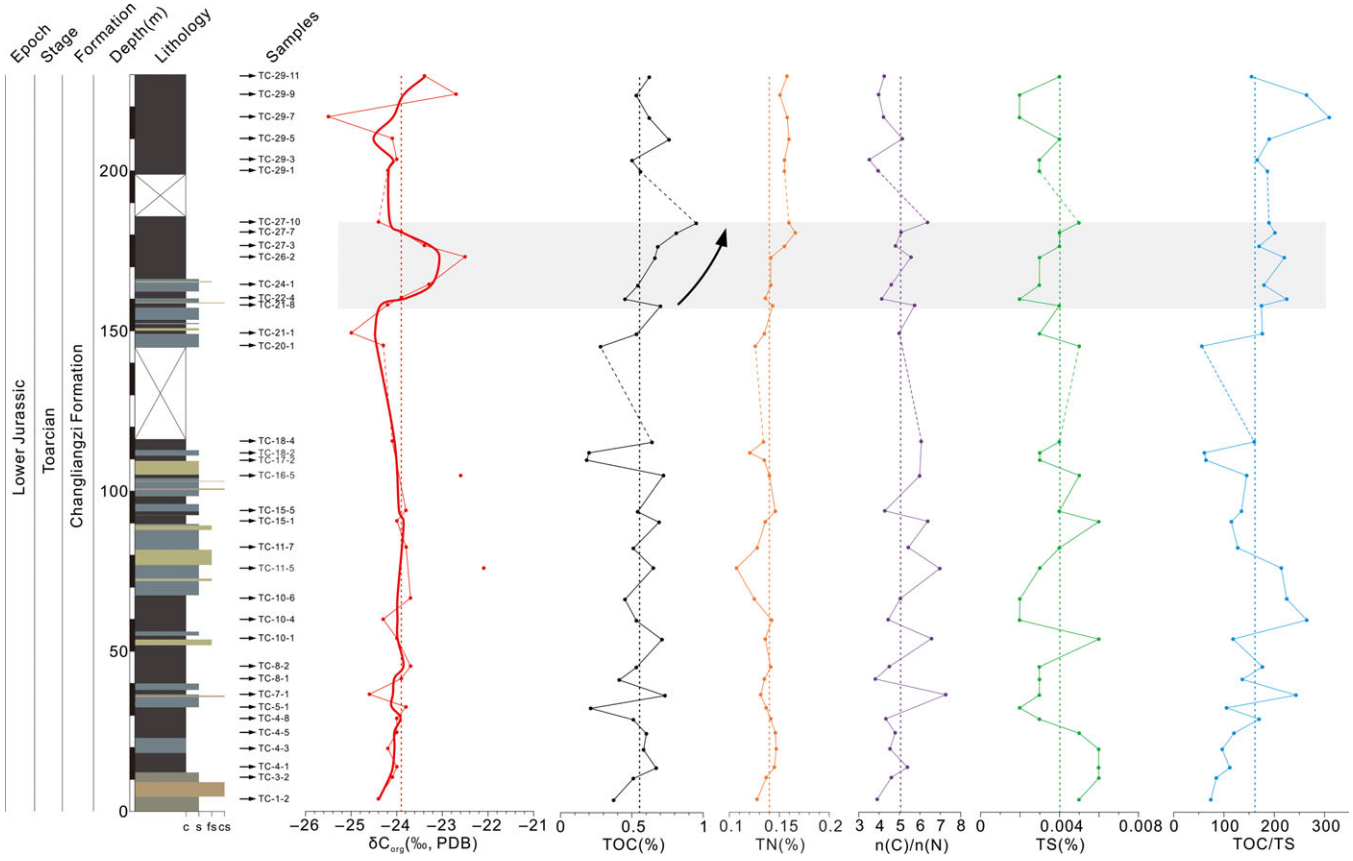

Fig. 3. (Colour online) Stratigraphic column of the Changliangzi section. Sample localities, organic carbon isotopes ($\delta^{13}C_{org}$) values, total organic carbon (TOC) contents, total nitrogen (TN) contents, total sulphur (TS) contents, atomic ratios of carbon to nitrogen (n(C)/n(N)), and ratios of total carbon and total sulphur (TOC/TS) are presented. Three-point moving averages of $\delta^{13}C_{org}$ are plotted in thick red lines. The grey block represents the segment with the $\delta^{13}C_{org}$ positive shift in the interval of *c.* 158–184 m. The vertical dotted lines represent the mean value of each parameter for the complete sedimentary succession. At the bottom of the stratigraphic column: c – clay; s – sand; fs – fine sand; cs – coarse sand.

https://doi.org/10.1017/S0016756820001235 Published online by Cambridge University Press

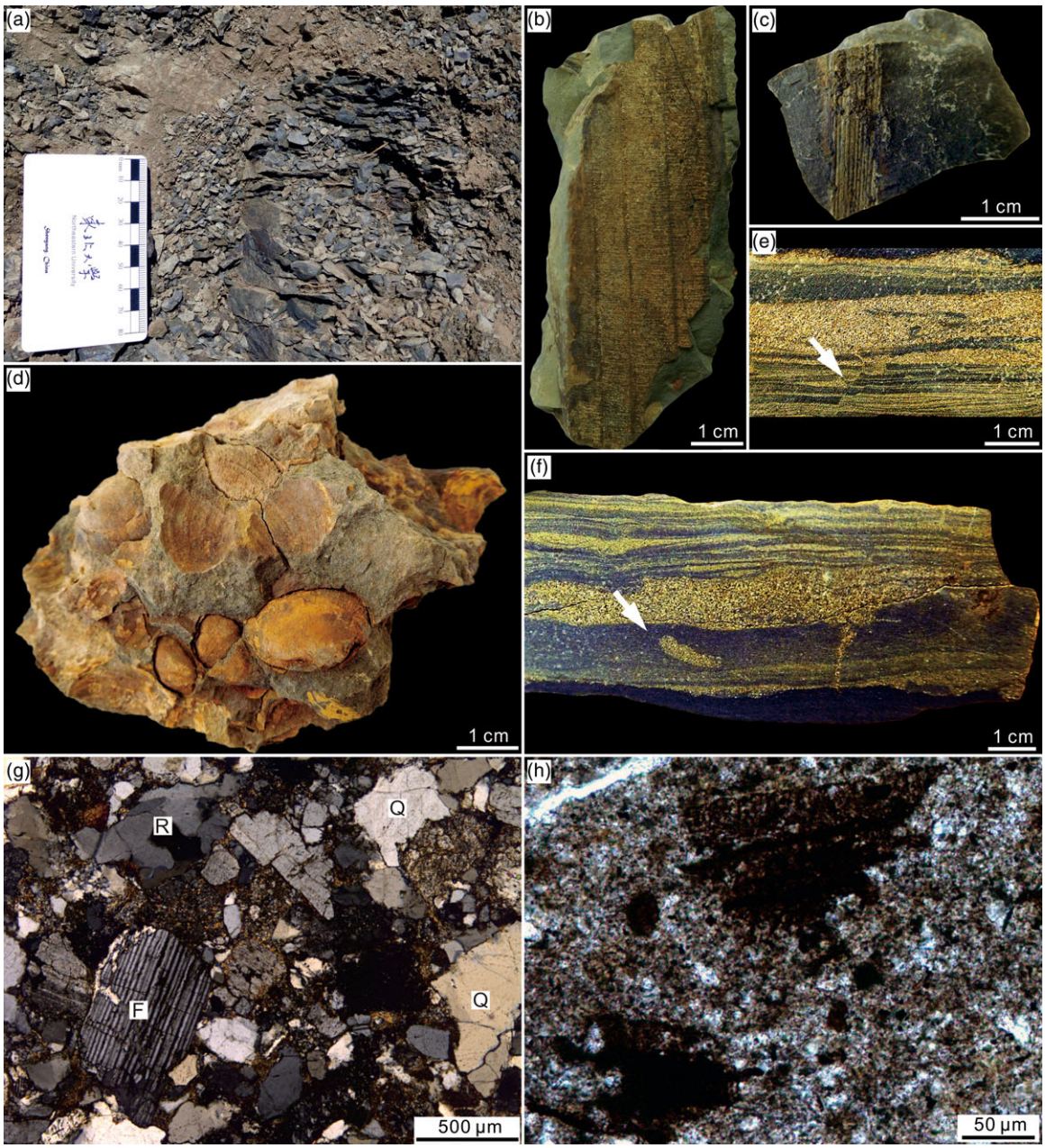

Fig. 4. (Colour online) Pictures of typical outcrop, hand specimen and micrographic image of the Changliangzi section. (a) Outcrop pictures exhibiting shale and siltstone, *c.* 26.80 m; (b, c) stalk fragments in siltstone from *c.* 54.50 m and 90.76 m, respectively; (d) well-preserved bivalves in fine sandstone from *c.* 104.78 m; (e, f) sedimentary structure in unfossiliferous fine sandstone from *c.* 88.71 m, where the white arrow in (e) and (f) indicates faulted lamina and sand-ball structure, respectively; (g) micrographic image of coarse sandstone from *c.* 8.70 m under crossed polars (Q – quartz; F –feldspar; R – rock debris); and (h) micrographic image of organic matter with residual plant structures in black shale from *c.* 169.56 m.

(14%) are similar to the above flora. Conifers are still lower in abundance (7%) and consist of *Pityophyllum* and *Elatocladus* (Fig. 7b).

4.c. Geochemical characteristics

There are distinct variations in the values of $\delta^{13}C_{org}$ and the content of TOC, TN and TS throughout the Changliangzi section (Fig. 3), ranging from −25.5‰ to −22.1‰ (average, −23.8‰), 0.18% to 0.95% (average, 0.56%), 0.104% to 0.186% (average, 0.139%) and 0.002% to 0.006% (average, 0.004%), respectively. The $\delta^{13}C_{org}$ remain close to the average and demonstrate only small fluctuations in the intervals of 0–158 m and 184–230 m of the Changliangzi section (Fig. 3). The positive shift of $\delta^{13}C_{org}$ is recorded in a 26-m-thick interval (158–184 m) and includes a maximum excursion of 1.3‰ compared with the average (Fig. 3). The TOC contents in the intervals of 0–158 m and 184–230 m fluctuate slightly between 0.37% and 0.73% (average, 0.57%) and 0.50% and 0.76% (average, 0.59%), respectively, with the exception of samples TC-5-1, TC-17-2, TC-18-2 and TC-20-1. These samples have excessively low TOC values that could be related to the relatively coarse-grained siltstone, which has a higher deposition rate. The TOC values in the interval of 158–184 m gradually increase in the range of 0.45–0.95% (average, 0.68%). There is no obvious trend for TN and TS. Significantly, the positive excursion of $\delta^{13}C_{org}$ and the increase in TOC content are

https://doi.org/10.1017/S0016756820001235 Published online by Cambridge University Press

Table 1. List and vertical distribution of the plant macrofossils in the Tianshifu Basin

Plant species	Changliangzi Formation	Dabu Formation
Ferns		
Dicksoniaceae		
Coniopteris tatungensis	+	+
Coniopteris burejensis	+	
Coniopteris gaojiatianensis	+	
Coniopteris hymenophylloides	+	
Coniopteris simplex		+
Coniopteris sp.		+
Dicksonia concinna		+
Marattiaceae		
Marattiopsis cf. *hoerensis*		+
Osmundaceae		
Cladophlebis asiatica	+	+
Cladophlebis delicatula	+	
Cladophlebis ichiinensis		+
Cladophlebis sp.		+
Todites cf. *shensiensis*		+
Todites williamsoni	+	+
Schizaeaceae		
Klukia cf. *exilis*	+	
Sphenopsids		
Equisetum guojiadianense	+	
Equisetum ilmijense		+
Equisetum laterale	+	+
Equisetum sibiricum	+	+
Neocalamites carrerei		+
Neocalamites cf. hoerensis		+
Neocalamites sp.	+	
Ginkgophytes		
Ginkgoales		
Baiera gracilis	+	+
Baira minima		+
Ginkgo sp.		+
Sphenarion latifolia		+
Sphenobaiera longifolia		+
Sphenobaiera sp.		+
Czekanowskiales		
Czekanowskia sp.		+
Cycadophytes		
Bennettiales		
Pterophullum longifolium	+	+
Pterophyllum angustum		+
Pterophyllum sp.		+
Cycadales		
Nilssonia acuminate		+
Nilssonia cf. *acuminate*	+	
Nilssonia sp.		+
Conifers		
Podozamitaceae		
Podozamites lanceolatus	+	
Uncertain genus		
Elatocladus sp.		+

accompanied by a variation in facies from shallow-lake to deep-lake, which indicates that there were environmental and/or climatic changes within the Tianshifu Basin.

In addition, the atomic ratios of TOC to TN (n(C)/n(N)) were calculated for their special significance in determining the sources of OM (Meyers, 1994, 2003). It should be noted that when sediments have a low OM content (TOC < 0.3%), atomic C/N ratios can be greatly depressed; the value of n(C)/n(N) then provides a misleading indication of the OM origin (Meyers, 1997). The data for samples TC-5-1, TC-17-2, TC-18-2 and TC-20-1 were therefore not considered to be appropriate for use in such calculations. For other samples, effective values of n(C)/n(N) range from 3.54 to 7.28 with an average value of 5.03 (Table 2). The TOC/TS ratios were calculated because sulphate reduction coupled with the oxidation of sedimentary organic matter would be reflected in the TOC/TS ratios (Wu *et al.* 2007*a*). The TOC/TS ratios fluctuate greatly from 56.00 to 310.00 with an average of 160.74 (Fig. 3; Table 2).

5. Discussion

5.a. Climate as inferred by flora

5.a.1. The climatic significance of flora

Interpretations of the continental climate are primarily based on the flora, which is considered to be very sensitive to environmental and climatic changes and is a useful palaeoecological and palaeoclimate proxy. Although no fossil plant samples of the early–middle Early Jurassic period have been found in the Tianshifu Basin in eastern Liaoning, plant assemblages do occur in the lower part of the Beipiao Formation in western Liaoning. In this study, ferns, cycadophytes, ginkgophytes, conifers and sphenopsids were identified from the material collected in the Tianshifu Basin. In addition to the plant fossils collected in this study, those genera and species recorded by previous researchers are also considered. Moreover, lycopsids and bryophytes were recorded in the Dabu Formation and the lower part of the Beipiao Formation, respectively (Zhang & Zheng, 1987; LBGMR, 1989; Zheng & Zhang, 1990*a*, *b*). The climatic implications of the plants involved in this study are described in the following (Table 3).

https://doi.org/10.1017/S0016756820001235 Published online by Cambridge University Press

Fig. 5. (Colour online) Pictures of phytolite in the Tianshifu Basin (Part I). Sample localities are represented by PL (phytolite locality) and the alphabetic code corresponds to that shown in Figure 1c. (a) *Pterophyllum* sp., Dabu Formation, PL-B; (b) *Coniopteris burejensis* (Zalessky) Seward, Changliangzi Formation, PL-A; (c) *Coniopteris gaojiatianensis* Zhang, Changliangzi Formation, PL-A; (d) *Podozamites lanceolatus* (Lindley et Hutton) Braun, lower Changliangzi Formation, PL-A; (e) *Equisetum sibiricum* (Heer), Changliangzi Formation, PL-A; (f) *Equisetum laterale* Phillips, Changliangzi Formation, PL-A; (g) *Todites* cf. *shensiensis* (Pán) Sze, Dabu Formation, PL-C; (h) *Sphenobaiera longifolia* (Pomer) Florin, Dabu Formation, PL-C; (i) *Equisetum ilmijense* (Prynada), Dabu Formation, PL-C; (j) *Elatocladus* sp., Dabu Formation, PL-B; (k) *Cladophlebis ichiinensis* Sze, Dabu Formation, PL-C; (l) *Coniopteris tatungensis* Sze, Dabu Formation, PL-B; (m) *Cladophlebis asiatica* Chow et Yeh, Dabu Formation, PL-B; and (n) *Cladophlebis delicatula* Yabe et Ôishi, Changliangzi Formation, PL-A.

Ferns were the main group of the Mesozoic flora, and had strict climatic and environmental requirements (Buatois *et al.* 2016). The different families preferred different environments: the Osmundaceae was mainly adapted to a warm and humid climate, while the Schizaeaceae, Marattiaceae and Dipteridaceae are generally regarded as good indicators of a tropical–subtropical climate (Vakhrameyev, 1991; Van Konijnenburg-Van Cittert, 2002). During Jurassic time, the Dicksoniaceae was abundant from the tropics to the poles (Deng, 2007); they are therefore not regarded as a useful Jurassic climate proxy. During Mesozoic time, Cycadales were distributed primarily in the tropical–subtropical zone and were adapted to a dry climate (Bomfleur *et al.* 2010; Sun *et al.* 2010). However, there were some cycad-like genera, such as *Anomozamites*, *Pterophyllum* and *Nilssonia*, that were more abundant in the temperate zone (Deng, 2007). The ginkgophytes were mainly restricted to temperate regions during Mesozoic time, indicating a seasonal climate (Vakhrameyev, 1991). However, the Czekanowskiales are believed to represent a relatively cold climate (Vakhrameyev, 1991; Bomfleur *et al.* 2010). Extant Conifers are widely distributed in temperate and cold zones. The Podozamitaceae, Taxodiaceae and the form genus *Elatocladus* generally indicate a temperate and humid climate, while many Pinaceous species can withstand severe cold (Wang *et al.* 2005; Pole, 2009; Bomfleur *et al.* 2010). Mesozoic sphenopsids mainly included *Neocalamites* and *Equisetites*, and were distributed globally but primarily found in warm regions (Deng, 2007; Zhang *et al.* 2014). Bryophytes usually grow under more or less humid conditions (Wang *et al.* 2005; Li *et al.* 2018). Lycopsids were relatively rare in the Mesozoic, with some adapted to a humid climate

https://doi.org/10.1017/S0016756820001235 Published online by Cambridge University Press

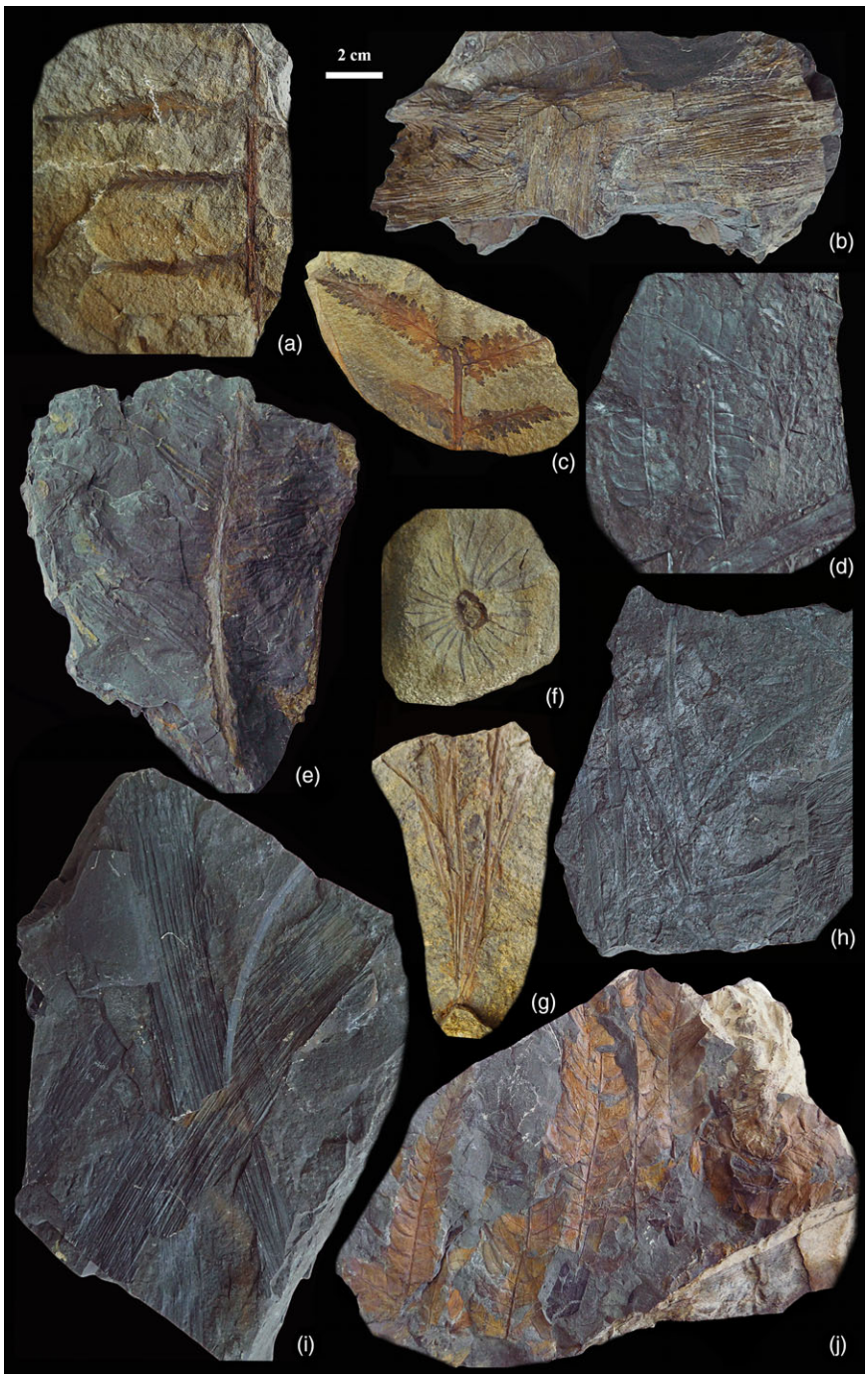

Fig. 6. (Colour online) Pictures of phytolite in the Tianshifu Basin (Part II). Sample localities are represented by PL (phytolite locality) and the alphabetic code corresponds to that shown in Figure 1c. (a) *Klukia* cf. *exilis* (Phillips, 1829) Raciborski 1890 emend. Harris, Changliangzi Formation, PL-A; (b) *Neocalamites* sp., Changliangzi Formation, PL-A; (c) *Coniopteris hymenophylloides* Brongniart, Changliangzi Formation, PL-A; (d) *Todites williamsoni* (Brongniart) Seward, Dabu Formation, PL-C; (e) *Nilssonia* sp., Dabu Formation, PL-B; (f) *Equisetum guojiadianense* Zhang et Zheng, Changliangzi Formation, PL-A; (g) *Sphenarion latifolia* (Turutanova-Ketova) Harris, Dabu Formation, PL-B; (h) *Pityophyllum longifolium* (Nathorst) Moeller, Dabu Formation, PL-C; (i) *Neocalamites* cf. *hoerensis* (Schimper) Halle, Dabu Formation, PL-C; and (j) *Todites williamsoni* (Brongniart) Seward, Changliangzi Formation, PL-A.

(e.g. *Lycopodites*) and others to drier conditions (Deng, 2007; Schrank, 2010).

5.a.2. Climate change during Early–Middle Jurassic time

According to the plant macrofossils (Table 3), the climate of the Early–Middle Jurassic period in eastern Liaoning can be indicated by computing the proportion of plant taxa (on a specimen basis) representing a temperate and humid, tropical–subtropical and moderate–cool climate (Fig. 8).

Within the lower–middle Lower Jurassic strata (the Beipiao Formation), plants that represent a temperate and humid climate had an absolute advantage (74%). The plants indicating a tropical–subtropical and moderate–cool climate were both rare and present in the same proportion (6%).

https://doi.org/10.1017/S0016756820001235 Published online by Cambridge University Press

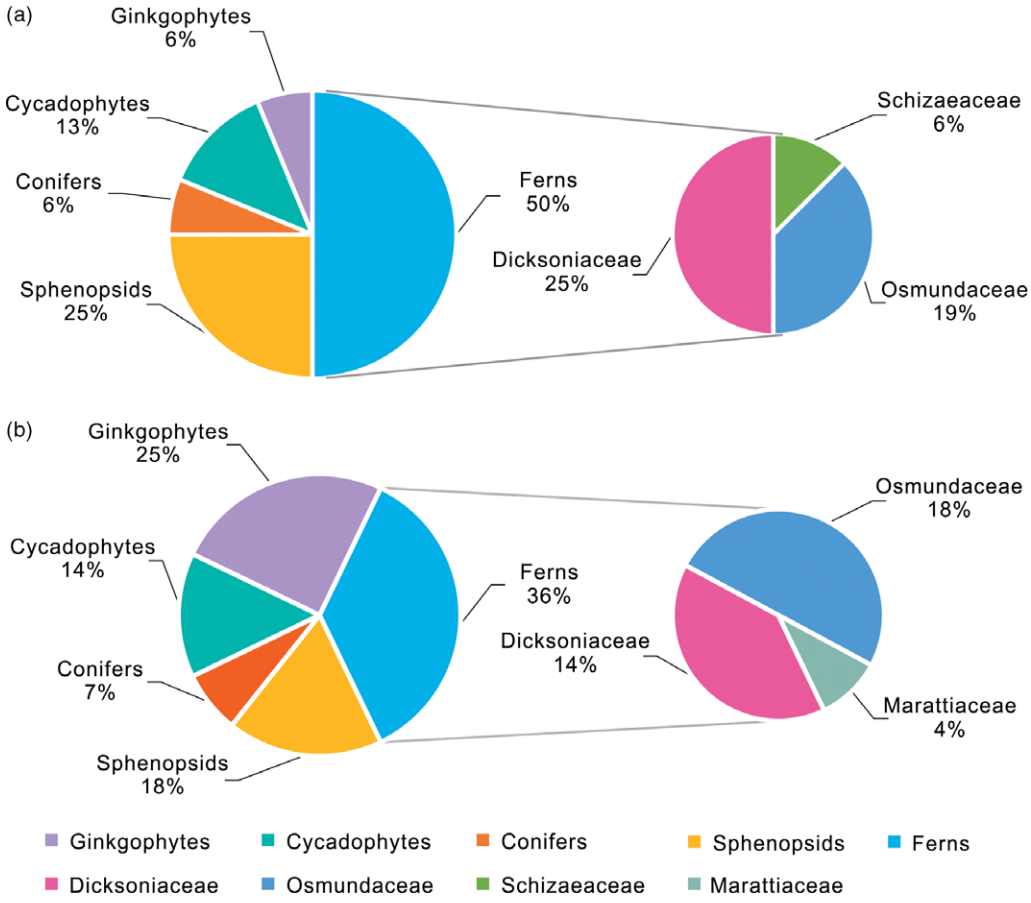

Fig. 7. (Colour online) Proportion of plant composition of the upper flora of the Changliangzi Formation and the Dabu Formation. It is revealed that the plant composition of the Dabu Formation is different from that of the upper part of the Changliangzi Formation, especially the significant increase in ginkgophytes, indicating a potential climate change. Floral composition of (a) the upper part of the Changliangzi Formation; and (b) the Dabu Formation.

Within the upper Lower Jurassic deposits (the upper part of the Changliangzi Formation), the temperate and humid climate still ruled, and the related plants accounted for 69% (73% in previous studies), while drought-resistant plants increased to 10% (in previous studies). Plants that represent a moderate–cool climate virtually disappeared.

The climate of the Middle Jurassic period was obviously different from that during the late Early Jurassic period. Plants that were adapted to a temperate and humid climate in the Dabu Formation increased to 75% (in this study) or 70% (in previous studies). Drought-tolerant plants of the Zhuanshanzi and Dabu formations were obviously less prevalent than those of the Changliangzi Formation, with a content of 5% (in previous studies) and 4% (in this study), respectively. Hekistotherms significantly increased to 9% (in previous studies) in the Zhuanshanzi Formation and 7% (in this study) and 6% (in previous studies) in the Dabu Formation.

It is obvious that plant groups that grow best under a temperate and humid climate dominated the whole flora, suggesting that this was the climate for eastern Liaoning during the Early–Middle Jurassic period. Although the proportion of plants that are more representative of hot and cool climates is relatively low, their climatic significance is still of great importance. Within the upper part of the Changliangzi Formation, there is an increase in the proportion of thermophilic plants and a decrease in the psychrophilic plants compared with the lower part of the Beipiao Formation (contemporaneous with the lower part of the Changliangzi Formation, but there are no isotopic data). Although the change in the proportion of plants is relatively small and the inferred difference in temperature was also small, this still suggests a warmer climate during the late Early Jurassic period in contrast to the earlier and later Jurassic periods.

5.b. Implications of geochemical characteristics

5.b.1. Organic matter: provenance and contents

Sedimentary organic matter (OM) may provide important information regarding the environment of palaeolakes, with the two most important being the source of the OM and the abundance of the biota that produced the OM (Meyers, 2003). Plants are the primary contributors to OM in lacustrine sediments (Meyers & Lallier-Vergès, 1999), and the types of plants that provide sedimentary OM largely affect interpretation of other geochemical indexes, especially the organic carbon isotope composition (Meyers, 1997, 2003). The provenance of OM should therefore be determined before the interpretation of changes in the organic carbon isotope composition.

The C/N ratios and organic carbon isotopes are regarded as reliable indicators for distinguishing the origin of sedimentary OM (whether phytoplankton or various land plants). These two indicators are widely applied in research on lacustrine or coastal environments (Meyers & Horie, 1993; Meyers, 1994). OM produced from atmospheric CO_2 by C_4 land plants usually contains an average

https://doi.org/10.1017/S0016756820001235 Published online by Cambridge University Press

Table 2. Lithology and results of organic carbon isotopes ($\delta^{13}C_{org}$), total organic carbon (TOC), total nitrogen (TN) and total sulphur (TS) analyses. Atomic ratios of TOC to TN (n(C)/n(N)) and ratios of TOC to TS (TOC/TS) were also calculated

Samples	$\delta^{13}C_{org}$ (‰, PDB)	TOC (%)	TN (%)	n(C)/n(N)	TS (%)	TOC/TS	Lithology
TC-1-2	−24.4	0.37	0.110	3.92	0.005	74.00	Yellow-green siltstone
TC-3-2	−24.1	0.51	0.129	4.61	0.006	85.00	Grey-green siltstone
TC-4-1	−24.0	0.67	0.145	5.39	0.006	111.67	Black shale
TC-4-3	−24.2	0.58	0.149	4.54	0.006	96.67	Black shale
TC-4-5	−24.0	0.60	0.146	4.79	0.005	120.00	Grey-black siltstone
TC-4-8	−24.0	0.51	0.137	4.34	0.003	170.00	Black shale
TC-5-1	−23.8	0.21	0.129	–	0.002	105.00	Yellow-green siltstone
TC-7-1	−24.6	0.73	0.117	7.28	0.003	243.33	Grey-black siltstone
TC-8-1	−23.9	0.41	0.125	3.83	0.003	136.67	Grey-black siltstone
TC-8-2	−23.7	0.53	0.137	4.51	0.003	176.67	Grey-green mudstone
TC-10-1	−24.0	0.71	0.126	6.57	0.006	118.33	Grey-green siltstone
TC-10-4	−24.3	0.53	0.139	4.45	0.002	265.00	Grey-green siltstone
TC-10-6	−23.7	0.45	0.104	5.05	0.002	225.00	Grey-black siltstone
TC-11-5	−22.1	0.64	0.107	6.98	0.003	213.33	Grey-green mudstone
TC-11-7	−23.8	0.51	0.110	5.41	0.004	127.50	Grey-green siltstone
TC-15-1	−24.0	0.69	0.126	6.39	0.006	115.00	Grey-black siltstone
TC-15-5	−23.8	0.54	0.147	4.29	0.004	135.00	Grey-green siltstone
TC-16-5	−22.6	0.72	0.140	6.00	0.005	144.00	Grey-black siltstone
TC-17-2	–	0.19	0.135	–	0.003	63.33	Grey-green siltstone
TC-18-2	–	0.18	0.121	–	0.003	60.00	Black shale
TC-18-4	−24.1	0.64	0.123	6.07	0.004	160.00	Black shale
TC-20-1	−24.3	0.28	0.106	–	0.005	56.00	Yellow-green siltstone
TC-21-1	−25.0	0.53	0.124	4.99	0.003	176.67	Grey-green siltstone
TC-21-8	−24.2	0.70	0.142	5.75	0.004	175.00	Black shale
TC-22-4	−23.9	0.45	0.127	4.13	0.002	225.00	Black shale
TC-24-1	−23.3	0.54	0.137	4.60	0.003	180.00	Grey-green siltstone
TC-26-2	−22.5	0.66	0.138	5.58	0.003	220.00	Grey-black siltstone
TC-27-3	−23.4	0.68	0.165	4.81	0.004	170.00	Black shale
TC-27-7	−23.9	0.81	0.186	5.08	0.004	175.00	Black shale
TC-27-10	−24.4	0.95	0.174	6.37	0.005	190.00	Black shale
TC-29-1	−24.2	0.56	0.165	3.96	0.003	186.67	Black shale
TC-29-3	−24.0	0.50	0.165	3.54	0.003	166.67	Black shale
TC-29-5	−24.1	0.76	0.173	5.13	0.004	190.00	Black shale
TC-29-7	−25.5	0.62	0.171	4.23	0.002	310.00	Black shale
TC-29-9	−22.7	0.53	0.155	3.99	0.002	265.00	Black shale
TC-29-11	−23.4	0.62	0.170	4.25	0.004	155.00	Black shale

$\delta^{13}C$ value of *c.* −14‰, and the $\delta^{13}C$ value of OM produced from atmospheric CO_2 by C_3 land plants and lacustrine algae is *c.* −27‰, on average. Protein-rich OM from lacustrine algae has C/N values that are commonly between 4 and 10, whereas protein-poor OM from land plants usually has C/N values of 20 or greater (Meyers, 1994). Atomic C/N ratios and the $\delta^{13}C_{org}$ of sediments from the Changliangzi section range from 3.54 to 7.28 and −25.5‰ to −22.1‰, respectively. These analytical results are in accordance with the geochemical characteristics of the OM obtained from aquatic algae. A discrimination diagram was compiled to combine the values of atomic C/N ratios and organic carbon isotopes (Meyers & Lallier-Vergès, 1999), and all points are found to fall in or near the range of lacustrine algae (Fig. 9). The OM is therefore determined as being predominantly derived from lacustrine algae.

The TOC concentration is a primary proxy for describing OM abundance, and the TOC contents are mainly controlled by the

https://doi.org/10.1017/S0016756820001235 Published online by Cambridge University Press

Table 3. Palaeoclimate types of major Early–Middle Jurassic plants in eastern Liaoning, mainly after Vakhrameyev (1991), Van Konijnenburg-Van Cittert (2002), Wang *et al.* (2005), Deng (2007), Pole (2009), Bomfleur *et al.* (2010), Schrank (2010), Sun *et al.* (2010), Zhang *et al.* (2014), and Li *et al.* (2018)

Climate type	Plant type[a]		
Temperate–humid climate	Bryophytes		
	Sphenopsids		*Neocalamites* + *Equisetites*
	Ferns	Osmundaceae	
	Cycadophytes	Bennettiales	*Anomozamites* + *Pterophyllum*
		Cycadales	*Nilssonia*
	Ginkgophytes	Ginkgoales	
	Lycopsids	Lycopodiaceae	*lycopodites*
	Conifers	Podozamitaceae	
		Taxodiaceae	
		Uncertain genus	*Elatocladus*
Tropical–subtropical climate	Ferns	Schizaeaceae	
		Marattiaceae	
		Dipteridaceae	
	Cycadophytes	Bennettiales	*Tyrmia*
		Cycadales	*Ctenis*
Moderate–cool climate	Ginkgophytes	Czekanowskiales	
	Conifers	Pinaceae	

[a]*Anomozamites*, *Lycopodites*, *Tyrmia* and *Ctenis* were not collected in this study, but were recorded by Zhang & Zheng (1987), LBGMR (1989) and Zheng & Zhang (1990*a*, *b*).

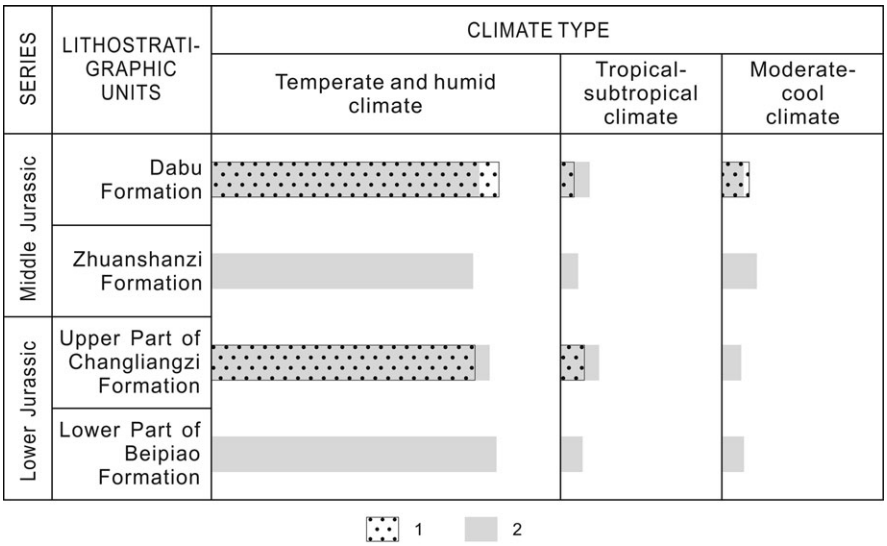

Fig. 8. Climate change diagram as inferred by flora. Based on the proportions of plant taxa, the upper part of the Changliangzi Formation (late Early Jurassic) was warmer than the lower part of the Beipiao Formation (early–middle Early Jurassic) and the Zhuanshanzi and Dabu formations (Middle Jurassic). Stippling – data from this study; shading – data from LBGMR (1989), Zhang & Zheng (1987), Zheng & Zhang (1990*b*).

initial production of biomass and the subsequent degree of degradation. An increasing TOC value generally means a rise in aquatic OM productivity and/or preservation (Meyers, 2003). In the Changliangzi section, the TOC contents of sediment in the interval of the $\delta^{13}C_{org}$ positive shift (158–184 m) gradually increase and are almost greater than average (Fig. 3). The high TOC values may indicate a high primary productivity or a high preservation of OM, or a combination of both. In the interval of 158–184 m, the TOC values correlate positively with the TN values (correlation coefficient of 0.6938, Fig. 10), suggesting that the contents of inorganic nitrogen are nearly constant (Talbot & Johannessen, 1992), so that the variations in TOC/TN can represent the changes in primary productivity. The increase in TOC contents is therefore not due to an increase in primary productivity, because there was no significant increase in

https://doi.org/10.1017/S0016756820001235 Published online by Cambridge University Press

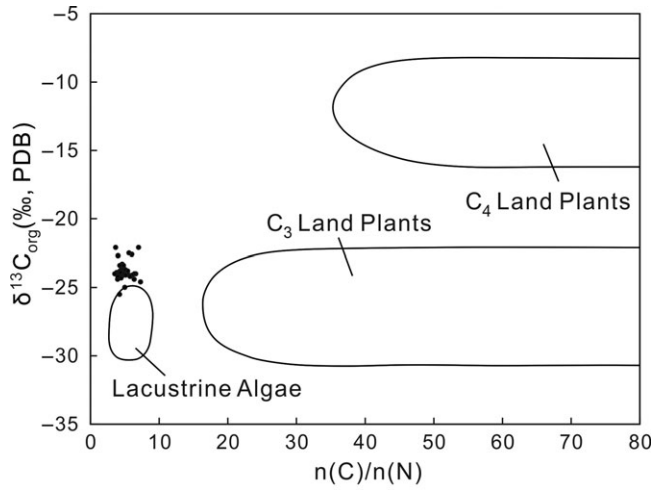

Fig. 9. Atomic C/N ratios (n(C)/n(N)) and organic carbon isotope ($\delta^{13}C_{org}$) identifiers of OM produced by lacustrine algae, C3 land plants and C4 land plants (Meyers & Lallier-Vergès, 1999). Data are from Table 2.

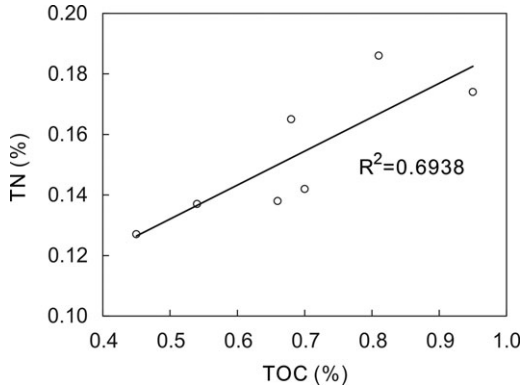

Fig. 10. Cross-plot of total nitrogen (TN) against total organic carbon (TOC) in the interval of 158–184 m in the Changliangzi section.

the TOC/TN ratios (Fig. 3). Furthermore, the correlation between TOC and TN indicates that the high values of TOC may be related to the high rates of OM preservation (Lebreton-Anberrée *et al.* 2016). The high TOC/TS ratios in the interval of 145–184 m also indicate a reducing environment because a higher TOC/TS ratio normally corresponds to stronger reduction conditions (Wu *et al.* 2007*a*) (Fig. 3). We therefore propose that the increase in OM in the interval of the $\delta^{13}C_{org}$ positive anomaly is attributed to the good preservation of OM rather than high primary productivity.

5.b.2. Driving factors of $\delta^{13}C_{org}$ shift

In a lacustrine system, the carbon isotope composition of depositional OM is primarily controlled by its sources and relates to the proportion of OM produced in a lake environment and derived from terrestrial input (Henderson & Holmes, 2009). In this study, the origin of sedimentary OM is considered stable and almost entirely formed from aquatic phytoplankton. The organic carbon isotope compositions therefore originate from within the lake and are related to the $\delta^{13}C$ of dissolved inorganic carbon utilized during photosynthesis. It is therefore considered that the changes in dissolved inorganic carbon are responsible for the $\delta^{13}C_{org}$ shift.

In a lake, the annual overturn of water and the rapid dissolution of biogenic carbonates maintain an equilibrium between atmospheric CO_2 and dissolved CO_2 (Meyers & Horie, 1993). Under equilibrium in lakes, phytoplankton generally preferentially use dissolved CO_2, while dissolved HCO will be used when the available dissolved CO_2 is limited (Meyers & Lallier-Vergès, 1999; Wang *et al.* 2013). The $\delta^{13}C$ value of algal OM could increase in the latter case because the dissolved HCO is characterized by a heavier carbon isotope ($\delta^{13}C$ *c.* 1‰) compared with dissolved CO_2 ($\delta^{13}C$ *c.* −7‰) (Meyers & Horie, 1993; Meyers, 1994).

Several changes in internal or external conditions can break this equilibrium and significantly affect the type and isotopic composition of dissolved inorganic carbon that is utilized by aquatic algae during photosynthesis. For example, high primary productivity can cause $\delta^{13}C_{org}$ to increase (Meyers & Horie, 1993). In addition, an increase in water temperature triggers rapid phytoplankton growth, and more dissolved inorganic carbon is assimilated, thereby resulting in a positive excursion of $\delta^{13}C_{org}$ (Wang *et al.* 2013). Meanwhile, the concentrations of dissolved CO_2 are lower in warmer waters (Rau *et al.* 1989); this leads to the selective uptake of isotopically heavier HCO by phytoplankton, which then produces a positive $\delta^{13}C_{org}$ bias. Moreover, aquatic plants have thicker and more stagnant boundary layers in low-turbulence lentic systems than in fast-moving water, thereby restraining the ability of the plants to obtain fresh carbon and promoting greater ^{13}C-depletion (France, 1995). Furthermore, an increase in the atmospheric partial pressure of CO_2 (pCO_2) causes a high equilibrium concentration of dissolved CO_2 in lakes, and consequently leads to a negative migration of $\delta^{13}C_{org}$ (Meyers & Horie, 1993).

We have shown that there is no significant change in primary productivity, so a productivity change can be ruled out as the reason for the positive migration of the $\delta^{13}C_{org}$. Furthermore, the effects of the increase in atmospheric pCO_2 that have been recorded elsewhere during late Early Jurassic time (McElwain *et al.* 2005) would cause a carbon isotope shift to a lighter isotopic ratio, not heavier. Therefore, the most likely cause of the positive shift of $\delta^{13}C_{org}$ recorded in this paper is climate warming. The warmer water could have produced algae blooms and a decline in the amount of dissolved CO_2, leading to a positive shift in the carbon isotope composition of algal OM. Furthermore, high temperature enhances lake stability (Jöhnk *et al.* 2008), and poor water circulation can promote a positive change in $\delta^{13}C_{org}$. The positive change in organic carbon isotopes of sediments in the Changliangzi section consequently appears to preserve a record of climate warming during the late Early Jurassic period.

5.c. Early Jurassic (Toarcian) climate events

In this study, the increase in plants representing a tropical–subtropical climate and the positive excursion of $\delta^{13}C_{org}$ recorded in the upper part of Changliangzi Formation both confirm that the Tianshifu Basin experienced a climatic warming event during the late Early Jurassic (Toarcian) period. This climate change is not restricted to the one basin, but can be distinguished in many regions in northern China. A marked decline in floral diversity and a conspicuous increase in thermophilic plants are well known in the lower Jurassic successions across northern China (Deng *et al.* 2012). There is even a considerable presence of drought-tolerant plants in NW China (Wu *et al.* 1986; Li *et al.* 1988), and a peak value in the percentage of *Classopollis* pollen is apparent during late Early Jurassic time, which also indicates a high temperature and a drought-prone climate (Wang *et al.* 2005; Yan *et al.* 2006; Tao *et al.* 2013; Yang *et al.* 2013). In addition, within the upper Lower Jurassic interval, the coal-bearing strata become interrupted by

https://doi.org/10.1017/S0016756820001235 Published online by Cambridge University Press

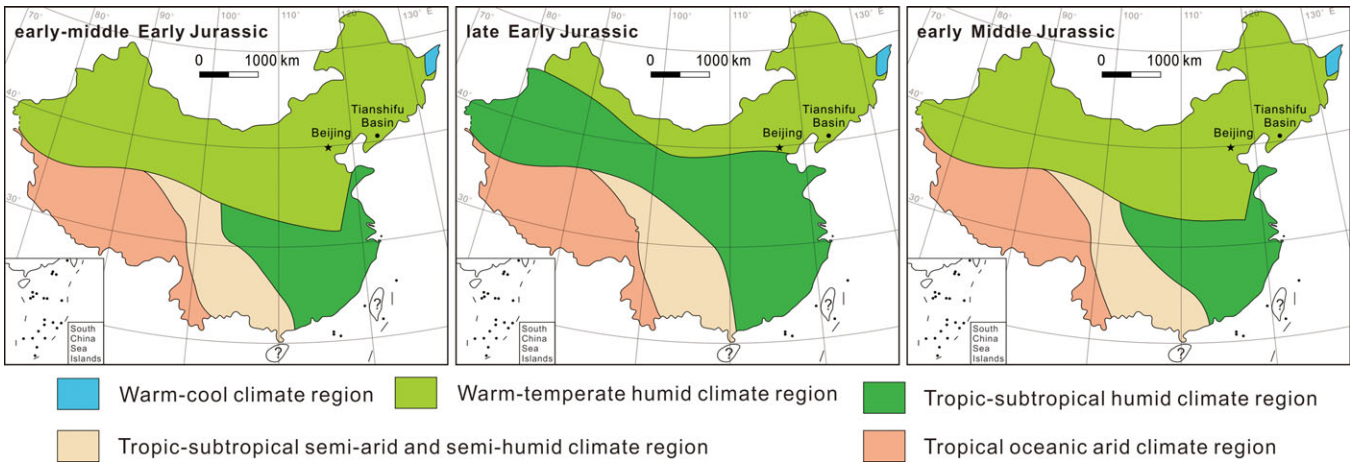

Fig. 11. (Colour online) The Early–Middle Jurassic climatic regions of China (after Deng *et al.* 2017).

coal-free strata, and the 'variegated' or 'red beds' that appeared only in southern China during the early Early Jurassic and Middle Jurassic periods also appear in northern China (Deng *et al.* 2012). Based on palaeontology, sedimentology and geochemistry, and the stomatal index and stomatal ratio of fossilized plants, Deng *et al.* (2017) (Fig. 11) found that the boundary of climate zones during the late Early Jurassic period moved towards the North Pole, in contrast to that during the early–middle Early Jurassic and early Middle Jurassic periods.

Moreover, the high percentage of *Classopollis* in early Jurassic successions of Siberia, Europe and central Asia (Vakhrameyev, 1982, 1991), rising marine temperatures in Europe (Suan *et al.* 2008; Dera *et al.* 2009), and intensified storm events and extreme warmth in the Tibetan Himalaya (Han *et al.* 2018) indicate that similar climatic events occurred globally. A raised atmospheric pCO_2 has been indicated by a short-lived negative carbon isotope excursion during Toarcian time and has been considered to be related to CO_2 released from the Karoo–Ferrar volcanism and methane from the dissociation of methane clathrate and magma-intrusion into Gondwana coals (Hesselbo *et al.* 2000; Svensen *et al.* 2004; Kemp *et al.* 2005; Burgess *et al.* 2015). Meanwhile, a sharp enhancement of atmospheric pCO_2 has also been recorded during research on terrestrial leaf stomatal density (McElwain *et al.* 2005). This suggests that large releases of greenhouse gas inevitably promoted warm greenhouse conditions during late Early Jurassic time. The climate change in the Tianshifu Basin and in other regions in northern China may therefore be in some way associated with the enhanced global greenhouse effect during the Toarcian Age. The increase in thermophilic plants and the positive carbon isotope excursion in the upper part of the Changliangzi Formation in the Tianshifu Basin are also likely to result from climate warming driven by the enhanced greenhouse effect.

6. Conclusion

The Tianshifu Basin in eastern Liaoning, NE China, contains a set of lacustrine sediments and abundant plant fossils of Early–Middle Jurassic age, allowing assessment of climate and biodiversity during a time of major global changes. The floral features indicate that eastern Liaoning was primarily characterized by temperate and humid conditions during the Early to Middle Jurassic period, but with a warming event during the latter part of the Early Jurassic period, possibly coeval with the Toarcian event. The Changliangzi section, representing the late Early Jurassic, shows a transformation from shallow-lake facies to deep-lake facies. A positive excursion of organic carbon isotopes correlates with the deepening of the palaeolake. We consider that high temperatures could be the primary driving factors of $\delta^{13}C_{org}$ positive migration; the positive change in organic carbon isotopes in this study therefore appears to be due to climate warming during late Early Jurassic time.

Furthermore, the climate warming reflected by the flora variations and the positive excursion of the $\delta^{13}C_{org}$ in the Tianshifu Basin is consistent with those climate events recorded in the marine and other continental sequences elsewhere, which are considered to be associated with the enhanced global greenhouse effect during late Early Jurassic time. The palaeobotanic and isotopic data resulting from this study therefore provide new continental evidence supporting global warming during late Early Jurassic time. It has been confirmed that the continental record of climate change complements the marine change, even though the record from land is still relatively scarce. Increased terrestrial data are consequently urgently needed to improve understanding of the Jurassic palaeoenvironment and palaeoclimate.

Acknowledgements. This research was funded by NSFC grants (nos 41972002 and 41172003). Lanzhou Center for Oil and Gas Resources, Institute of Geology and Geophysics, Chinese Academy of Sciences and Nanjing Institute of Geography and Limnology, Chinese Academy of Sciences are thanked for the geochemical analyses of sediments. We are also grateful for the comments of editors and reviewers, which significantly improved the manuscript.

References

Aberhan M and Baumiller TK (2003) Selective extinction among Early Jurassic bivalves: a consequence of anoxia. *Geology* **31**, 1077–80.

Al-Suwaidi AH, Angelozzi GN, Baudin F, Damborenea SE, Hesselbo SP, Jenkyns HC, Manceñido MO and Riccardi AC (2010) First record of the Early Toarcian Oceanic Anoxic Event from the Southern Hemisphere, Neuquén Basin, Argentina. *Journal of the Geological Society* **167**, 633–36.

Berner RA and Kothavala Z (2001) GEOCARB III: a revised model of atmospheric CO2 over Phanerozoic time. *American Journal of Science* **301**, 182–204.

Bomfleur B, Pott C and Kerp H (2010) Plant assemblages from the Shafer Peak Formation (Lower Jurassic), north Victoria Land, Transantarctic Mountains. *Antarctic Science* **23**, 188–208.

Buatois LA, Labandeira CC, Mángano MG, Cohen A and Voigt S (2016) The Mesozoic Lacustrine Revolution. In *The Trace-Fossil Record of Major Evolutionary Events* (eds MG Mángano and LA Buatois) pp. 179–263. Dordrecht: Springer.

https://doi.org/10.1017/S0016756820001235 Published online by Cambridge University Press

Burgess SD, Bowring SA, Fleming TH and Elliot DH (2015) High-precision geochronology links the Ferrar Large Igneous Province with early-Jurassic ocean anoxia and biotic crisis. *Earth and Planetary Science Letters* **415**, 90–99.

Chang SC, Zhang HC, Hemming SR, Mesko GT and Fang Y (2014) 40Ar/39Ar age constraints on the Haifanggou and Lanqi formations: when did the first flowers bloom? In *Sediment-Body Geometry and Heterogeneity: Analogue Studies for Modelling the Subsurface* (eds AW Martinius, JA Howell and TR Good), pp. 277–84. Geological Society of London, Special Publication no. 378.

Deng SH (2007) Palaeoclimatic implications of main fossil plants of the Mesozoic. *Journal of Palaeogeography* **9**, 559–74.

Deng SH, Lu YZ, Fan R, Fang LH, Li X and Liu L (2012) Toarcian (Early Jurassic) Oceanic Anoxic Event and the responses in terrestrial ecological system. *Earth Science-Journal of China University of Geosciences* **37**, 23–38.

Deng SH, Lu YZ, Zhao Y, Fan R, Wang YD, Yang XJ, Li X and Sun BN (2017) The Jurassic palaeoclimate regionalization and evolution of China. *Earth Science Frontiers* **24**, 106–42.

Dera G, Brigaud B, Monna F, Laffont R, Pucéat E, Deconinck JF, Pellenard P, Joachimski MM and Durlet C (2011) Climatic ups and downs in a disturbed Jurassic world. *Geology* **39**, 215–18.

Dera G, Pellenard P, Neige P, Deconinck JF, Puceat E and Dommergues JL (2009) Distribution of clay minerals in Early Jurassic Peritethyan seas: palaeoclimatic significance inferred from multiproxy comparisons. *Palaeogeography, Palaeoclimatology, Palaeoecology* **271**, 39–51.

Erba E, Bottini C, Faucher G, Gambacorta G and Visentin S (2019) The response of calcareous nannoplankton to oceanic anoxic events: the Italian pelagic record. *Bollettino Della Societa Paleontologica Italiana* **58**, 51–71.

France RL (1995) C-13 enrichment in benthic compared to planktonic algae - foodweb implications. *Marine Ecology Progress Series* **124**, 307–12.

Fu XG, Wang M, Zeng SQ, Feng XL, Wang D and Song CY (2017) Continental weathering and palaeoclimatic changes through the onset of the Early Toarcian Oceanic Anoxic Event in the Qiangtang Basin, eastern Tethys. *Palaeogeography, Palaeoclimatology, Palaeoecology* **487**, 241–50.

Han Z, Hu XM, Kemp DB and Li J (2018) Carbonate-platform response to the Toarcian Oceanic Anoxic Event in the Southern Hemisphere: implications for climatic change and biotic platform demise. *Earth and Planetary Science Letters* **489**, 59–71.

Henderson ACG and Holmes JA (2009) Palaeolimnological evidence for environmental change over the past millennium from Lake Qinghai sediments: a review and future research prospective. *Quaternary International* **194**, 134–47.

Hesselbo SP, Gröcke DR, Jenkyns HC, Bjerrum CJ, Farrimond P, Morgans Bell HS and Green OR (2000) Massive dissociation of gas hydrate during a Jurassic oceanic anoxic event. *Nature* **406**, 392–5.

Hesselbo SP and Pieńkowski G (2011) Stepwise atmospheric carbon-isotope excursion during the Toarcian Oceanic Anoxic Event (Early Jurassic, Polish Basin). *Earth and Planetary Science Letters* **301**, 365–72.

Jenkyns HC (1985) The early Toarcian and Cenomanian-Turonian Anoxic Events in Europe: comparisons and contrasts. *Geologische Rundschau* **74**, 505–18.

Jenkyns HC (1988) The early Toarcian (Jurassic) Anoxic Event; stratigraphic, sedimentary and geochemical evidence. *American Journal of Science* **288**, 101–51.

Jenkyns HC (2003) Evidence for rapid climate change in the Mesozoic-Palaeogene greenhouse world. *Philosophical Transactions of the Royal Society A-Mathematical Physical and Engineering Sciences* **361**, 1885–916.

Jöhnk KD, Huisman J, Sharples J, Sommeijer B and Stroom JM (2008) Summer heatwaves promote blooms of harmful cyanobacteria. *Global Change Biology* **14**, 495–512.

Kemp DB, Coe AL, Cohen AS and Schwark L (2005) Astronomical pacing of methane release in the Early Jurassic period. *Nature* **437**, 396–99.

Lebreton-Anberrée J, Li SH, Li SF, Spicer RA, Zhang ST, Su T, Deng CL and Zhou ZK (2016) Lake geochemistry reveals marked environmental change in Southwest China during the Mid Miocene Climatic Optimum. *Science Bulletin* **61**, 897–910.

Li LQ, Wang YD, Vajda V and Liu ZS (2018) Late Triassic ecosystem variations inferred by palynological records from Hechuan, southern Sichuan Basin, China. *Geological Magazine* **155**, 1793–810.

Li PJ, He YL, Wu XW, Mei SW and Li BY (1988) *Early to Middle Jurassic Strata and Flora in the Northeast Margin of Qaidam Basin, Qinghai Province*. Nanjing: Nanjing University Press.

Liaoning Bureau of Geology and Mineral Resources (LBGMR) (1989) *Regional Geology of Liaoning Province*. Beijing: Geology Press.

McArthur JM, Donovan DT, Thirlwall MF, Fouke BW and Mattey D (2000) Strontium isotope profile of the early Toarcian (Jurassic) Oceanic Anoxic Event, the duration of ammonite biozones, and belemnite palaeotemperatures. *Earth and Planetary Science Letters* **179**, 269–85.

McElwain JC, Wade-Murphy J and Hesselbo SP (2005) Changes in carbon dioxide during an oceanic anoxic event linked to intrusion into Gondwana coals. *Nature* **435**, 479–82.

Meyers PA (1994) Preservation of elemental and isotopic source identification of sedimentary organic matter. *Chemical Geology* **114**, 289–302.

Meyers PA (1997) Organic geochemical proxies of paleoceanographic, paleolimnologic, and paleoclimatic processes. *Organic Geochemistry* **27**, 213–50.

Meyers PA (2003) Applications of organic geochemistry to paleolimnological reconstructions: a summary of examples from the Laurentian Great Lakes. *Organic Geochemistry* **34**, 261–89.

Meyers PA and Horie S (1993) An organic carbon isotopic record of glacial-postglacial change in atmospheric pCO_2 in the sediments of Lake Biwa, Japan. *Palaeogeography, Palaeoclimatology, Palaeoecology* **105**, 171–78.

Meyers PA and Lallier-Vergès E (1999) Lacustrine sedimentary organic matter records of Late Quaternary paleoclimates. *Journal of Paleolimnology* **21**, 345–72.

Palliani RB, Mattioli E and Riding JB (2002) The response of marine phytoplankton and sedimentary organic matter to the Early Toarcian (Lower Jurassic) Oceanic Anoxic Event in northern England. *Marine Micropaleontology* **46**, 223–45.

Phillips J (1829) *Illustrations of the geology of Yorkshire; or, a description of the strata and organic remains of the Yorkshire Coast*. York: printed for the author by T Wilson.

Pole M (2009) Vegetation and climate of the New Zealand Jurassic. *GFF* **131**, 105–11.

Raciborski M (1890) Über die Osmundaceen und Schizaeaceen der Juraformation. *Botanische Jahrbucher* **13**, 1–9.

Rau GH, Takahashi T and Des Marais DJ (1989) Latitudinal variations in plankton $\delta^{13}C$: implications for CO_2 and productivity in past oceans. *Nature* **341**, 516–18.

Ros-Franch S, Echevarria J, Damborenea SE, Mancenido MO, Jenkyns HC, Al-Suwaidi A, Hesselbo SP and Riccardi AC (2019) Population response during an oceanic anoxic event: the case of Posidonotis (Bivalvia) from the Lower Jurassic of the Neuquen Basin, Argentina. *Palaeogeography, Palaeoclimatology, Palaeoecology* **525**, 57–67.

Ruban DAR (2004) Diversity dynamics of Early-Middle Jurassic brachiopods of Caucasus, and the Pliensbachian-Toarcian mass extinction. *Acta Palaeontologica Polonica* **40**, 275–82.

Ruebsam W, Müller T, Kovács J, Pálfy J and Schwark L (2018) Environmental response to the early Toarcian carbon cycle and climate perturbations in the northeastern part of the West Tethys shelf. *Gondwana Research* **59**, 144–58.

Schrank E (2010) Pollen and spores from the Tendaguru Beds, Upper Jurassic and Lower Cretaceous of southeast Tanzania: palynostratigraphical and paleoecological implications. *Palynology* **34**, 3–42.

Scotese CR (2004) A continental drift flipbook. *Journal of Geology* **112**, 729–41.

Shao JA and Yang W (2008) The age of volcanic rocks of the Xinglonggou Formation in Beipiao, western Liaoning, China: revisited. *Geological Bulletin of China* **27**, 912–16.

Slater SM, Twitchett RJ, Danise S and Vajda V (2019) Substantial vegetation response to Early Jurassic global warming with impacts on oceanic anoxia. *Nature Geoscience* **12**, 462–68.

Suan G, Mattioli E, Pittet B, Mailliot S and Lécuyer C (2008) Evidence for major environmental perturbation prior to and during the Toarcian (Early Jurassic) Oceanic Anoxic Event from the Lusitanian Basin, Portugal. *Paleoceanography* **23**, PA1202.

Sun CL, Tao L, Sun YW, Chen YJ, Li CT and Zhao GW (2010) Early Jurassic fossil cycads from Yihe Basin in southern Jilin province: paleoclimatic significance. *Geology and Resources* **19**, 5–12.

https://doi.org/10.1017/S0016756820001235 Published online by Cambridge University Press

Svensen HH, Planke S, Malthe-Sørenssen A and Jamtveit B (2004) Release of methane from a volcanic basin as a mechanism for initial Eocene global warming. *Nature* **429**, 542–45.

Talbot MR and Johannessen T (1992) A high resolution palaeoclimatic record for the last 27,500 years in tropical West Africa from the carbon and nitrogen isotopic composition of lacustrine organic matter. *Earth & Planetary Science Letters* **110**, 23–37.

Tao MH, Cui ZQ and Chen GQ (2013) Mesozoic sporo-pollen assemblages and climate fluctuations in Northeast China. *Acta Micropalaeontologica Sinica* **30**, 275–87.

Vajda V, Pole M and Sha J (2016) Mesozoic ecosystems – climate and biotas. *Palaeogeography, Palaeoclimatology, Palaeoecology* **464**, 1–4.

Vakhrameyev VA (1982) Classopollis pollen as an indicator of Jurassic and Cretaceous climate. *International Geology Review* **24**, 1190–96.

Vakhrameyev VA (1991) *Jurassic and Cretaceous Floras and Climates of the Earth*. Cambridge: Cambridge University Press.

Van Konijnenburg-Van Cittert JHA (2002) Ecology of some Late Triassic to Early Cretaceous ferns in Eurasia. *Review of Palaeobotany and Palynology* **119**, 113–24.

Wang BL, Liu CQ, Peng X and Wang FS (2013) Mechanisms controlling the carbon stable isotope composition of phytoplankton in karst reservoirs. *Journal of Limnology* **72**, 127–39.

Wang YD, Mosbrugger V and Zhang H (2005) Early to Middle Jurassic vegetation and climatic events in the Qaidam Basin, northwest China. *Palaeogeography, Palaeoclimatology, Palaeoecology* **224**, 200–16.

Wu XW, He YL and Mei SW (1986) Discovery of Ephedrites in Xiaoliangou Formation of lower Jurassic, Qinghai Province. *Acta Palaeobotany and Palynology Sinica*, 13–22.

Wu YH, Andreas L, Bernd W, Li SJ and Wang SM (2007a) Holocene climate change in the Central Tibetan Plateau inferred by lacustrine sediment geochemical records. *Science in China Series D: Earth Sciences* **50**, 1548–55.

Wu ZP, Hou XB and Li W (2007b) Discussion on Mesozoic Basin patterns and evolution in the eastern North China Block. *Geotectonica et Metallogenia* **31**, 385–99.

Xu K, Yang JG, Tao MH, Liang HD, Zhao CB, Li RH, Kong H, Li Y, Wan CB and Peng WS (2003) *Jurassic System in the North of China: Northeast Stratigraphic Region*. Beijing: Petroleum Industry Press.

Yan CF, Yuan JY, Zhao YC, Wei DT and Li ZG (2006) Jurassic spora-pollen assemblages and paleoclamate ininnermongolia, Gansu, Qinghai, China. *Natural Gas Geoscience* **17**, 634–39.

Yang B, Zhang XH, Ge MC and Pan WJ (2013) Discovery of sporopollen fossils of Jurassic Hongqi Formation in Xilinhot, Inner Mongolia, and its paleoclimate significance. *Geological Science and Technology Information* **32**, 143–47.

Zhang MZ, Dai S, Heimhofer U, Wu MX, Wang ZX and Pan BT (2014) Palynological records from two cores in the Gongpoquan Basin, central East Asia: evidence for floristic and climatic change during the Late Jurassic to Early Cretaceous. *Review of Palaeobotany and Palynology* **204**, 1–17.

Zhang W and Zheng SL (1987) Early Mesozoic fossil plants in western Liaoning, northeast China. In *Mesozoic Stratigraphy and Palaeontology in Western Liaoning* (eds XH Yu, WLWang and XT Liu), pp. 239–368. Beijing: Geology Press.

Zheng SL and Zhang W (1990a) Basic characteristics of Tianshifu Flora. *Liaoning Geology* 4, 322–34.

Zheng SL and Zhang W (1990b) Early and Middle Jurassic fossil flora from Tianshifu Liaoning. *Liaoning Geology* 3, 212–36.

Zhou N, Wang YD and McElwain JC (2018) Paleoclimate variations and paleo-CO2 change during the Toarcian (Early Jurassic) based on South China floras. In *Joint Meetings on the 12th National Congress of the Palaeontological Society of China (PSC) and the 29th Annual Conference of PSC*. Zhengzhou: Palaeontological Society of China, p. 90.

https://doi.org/10.1017/S0016756820001235 Published online by Cambridge University Press